*International Conference on Mathematics, Computational Methods & Reactor Physics (M&C 2009)*
Saratoga Springs, New York, May 3-7, 2009, on CD-ROM, American Nuclear Society, LaGrange Park, IL (2009)

# CRITICALITY ACCIDENT ALARM SYSTEM MODELING WITH SCALE

**Douglas E. Peplow and Lester M. Petrie, Jr.**
Oak Ridge National Laboratory
P.O. Box 2008, Bldg. 5700, Oak Ridge, TN 37831-6170
peplowde@ornl.gov; petrielmjr@ornl.gov

## ABSTRACT

Criticality accident alarm systems (CAAS) can be difficult to analyze because they consist of both criticality calculations and deep-penetration radiation transport calculations. Radiation transport codes are typically optimized for one of these two aspects but not both. A three-dimensional CAAS modeling capability within SCALE 6 has been created by linking the KENO-VI criticality code to the MAVRIC shielding sequence. KENO-VI has been optimized for criticality calculations and used for more than 20 years. MAVRIC (Monaco with Automated Variance Reduction using Importance Calculations) is a new sequence in SCALE 6 designed for radiation transport in deep-penetration problems. MAVRIC contains features such as automated variance reduction and mesh tally capabilities, which are quite useful in CAAS modeling.

*Key Words*: criticality, alarm system, variance reduction

## 1. INTRODUCTION

A wide variety of methods are currently used to calculate the response of criticality accident alarm systems (CAAS). Fast, approximate techniques typically model the criticality source as a point source and make use of one-dimensional, point-kernel, or build-up factor approximations for estimating transport over long distances and through thick shielding. Multi-dimensional discrete ordinates methods have been widely used [1,2] but require separate calculation of the critical system and the shielding systems as well as geometric approximations due to the orthogonal mesh.

Standard Monte Carlo codes using detailed models and detailed physics can be used for more accurate radiation transport simulations compared to point-kernel or build-up factor codes but can suffer from the long run times required to calculate detector responses with reasonably low levels of stochastic uncertainty. This is especially true for simulating systems that require tallies at many points, such as CAAS problems with multiple detectors. Similarly, Monte Carlo codes can accurately model the complex geometry necessary for CAAS problems, but typical variance reduction techniques are tailored to criticality or shielding problems, and as a result, CAAS problems are broken into multiple steps which can be unnecessarily complicated.

Many variance reduction methods have been used by Monte Carlo codes to reduce calculation times, but many of these involve iteration and a great deal of experience on the part of the user. Over the past decade, progress has been made developing hybrid methods that use approximate discrete ordinates solutions to generate space- and energy-dependent weight windows [3,4]—one of the most effective variance reduction techniques. These hybrid approaches have been used to

greatly improve calculation times for challenging Monte Carlo problems and have been automated in MCNP (Monte Carlo N-Particle) [5] and the MAVRIC (Monaco with Automated Variance Reduction using Importance Calculations) sequence in SCALE [6]—reducing the burden on the user. Both of these automated systems use the CADIS method—Consistent Adjoint Driven Importance Sampling—which forms an importance map and biased source distribution from the results of a coarse-mesh adjoint discrete ordinates calculation. The ADVANTG (Automated Deterministic VAriaNce reducTion Generator) system uses the TORT (Three-Dimensional Oak Ridge Radiation Transport) $S_N$ code and MCNP. The MAVRIC sequence in SCALE 6 uses the new functional modules Denovo, an $S_N$ code using a Koch-Baker-Alcouffe parallel sweep algorithm and nonstationary Krylov methods, and Monaco, a derivative of the MORSE (Multigroup Oak Ridge Stochastic Experiment) multigroup Monte Carlo code with many additions and improvements.

Recent work with MAVRIC has demonstrated [7,8] that an importance map and biased source distribution can be formed that will calculate multiple tallies or a large mesh tally with low relative uncertainties simultaneously. This extension of CADIS uses the results of a forward discrete ordinates calculation to form the source for the adjoint calculation. This approach, called forward-weighted CADIS (or FW-CADIS [9]), was implemented through the ADVANTG patch to MCNP5 and demonstrated the ability to calculate dose rates that ranged over 20 orders of magnitude across the various buildings of a pressurized-water-reactor (PWR) facility due to the operating reactor core [10]. In MAVRIC, the implementation of FW-CADIS has been completely automated. MAVRIC calculations of neutron transport through a three-section concrete labyrinth using FW-CADIS compared well to experimental measurements [11].

This paper details a new capability in SCALE 6 specifically made for simulating CAAS. The KENO-VI criticality code produces a fission source distribution that can be used by the MAVRIC sequence. The automated variance reduction in MAVRIC can transport these source particles through the critical materials and throughout the building, yielding an accurate simulation of CAAS problems in reasonable times.

## 2. METHODS

The CAAS capability in SCALE 6 is a two-step approach using KENO-VI and MAVRIC. The first step is the determination of the source distribution, typically done with the CSAS6 (Criticality Safety Analysis Sequence) control sequence, which uses the KENO-VI functional module. Along with calculating the system $k_{eff}$, KENO-VI has been modified to accumulate the fission distribution over the nonskipped generations. This information is collected on a three-dimensional Cartesian mesh that overlays the physical geometry model and is saved as a Monaco mesh source.

The mesh source is then used in the second step as a source term in MAVRIC. The absolute source strength is set by the user based on the total number of fissions (based on the total power released) during the criticality excursion. Further neutron multiplication is prevented in the MAVRIC transport calculation. If further fissions were allowed, Monaco would add neutrons to its particle bank faster than they could be removed (since the system is at or above critical) and would never finish.

The user can also tell MAVRIC to add fission photons to the mesh source, specifying which isotope to use for the multiplicity (photons per fission) and fission photon energy distribution. To correctly account for the number of source photons released per source neutron, the system $\bar{\nu}$ (neutrons per fission) calculated by KENO-VI is used. Measured data for real fission photon spectra are largely lacking. The ENDF/B-VII.0 (Evaluated Nuclear Data File B, Version VII, Release 0) data include only 23 isotopes with fission photon data, listed in Table I. These 23 isotopes use one of five different emission distributions, which are shown in Figure 1. Adding fission photons to the neutron source is optional; for example, in modeling neutron-only detectors, adding and following the fission photons in the transport calculation would only slow things down.

For the transport part, MAVRIC can be optimized to calculate one specific detector response at one location using CADIS or to calculate multiple responses/locations with roughly the same relative uncertainty using FW-CADIS. For calculating mesh tallies of fluxes or dose rates, MAVRIC also uses FW-CADIS to help balance the Monaco Monte Carlo calculation such that low flux voxels are computed with about the same relative uncertainty as the high flux voxels.

With this two-step approach, users will have a great deal of flexibility in modeling CAAS problems. The CSAS6 step and the MAVRIC step could both use the same geometry and materials definitions or could have different levels of detail included in each. For best results, a possible scheme would be to model the critical system geometry with only the closest surrounding materials but in fine detail. The transport geometry could leave out small details but would include the large building-level components. The fission source distribution from one CSAS6 calculation could be used in a number of different MAVRIC building/detector models, with each MAVRIC calculation optimized for a given type of detector.

**Table I. Fission photon multiplicity and distributions in ENDF/B-VII.0**

| ZAID | mult. | up to energy (eV) | dist. |
|---|---|---|---|
| 92232 | 8.18 | 30000000 | 1 |
| 92233 | 6.31 | 1090000 | 4 |
| 92234 | 8.18 | 30000000 | 1 |
| 92235 | 7.0437 | 1090000 | 2 |
| 92236 | 8.18 | 30000000 | 1 |
| 92237 | 8.18 | 30000000 | 1 |
| 92238 | 7.5326 | 30000000 | 1 |
| 92239 | 8.18 | 30000000 | 1 |
| 92240 | 8.18 | 30000000 | 1 |
| 92241 | 8.18 | 30000000 | 1 |
| 93237 | 7.17 | 549230 | 2 |
| 94239 | 7.7833 | 1090000 | 4 |
| 94240 | 8.095 | 1090000 | 4 |
| 94241 | 8.18 | 99990.01 | 1 |
| 94242 | 7.1 | 300000 | 5 |
| 94243 | 8.18 | 20000000 | 1 |
| 95241 | 7.1 | 30000000 | 3 |
| 95243 | 7.1 | 300000 | 5 |
| 96242 | 7.1 | 300000 | 5 |
| 96248 | 8.18 | 20000000 | 1 |
| 98250 | 8.18 | 20000000 | 1 |
| 98251 | 8.18 | 20000000 | 1 |

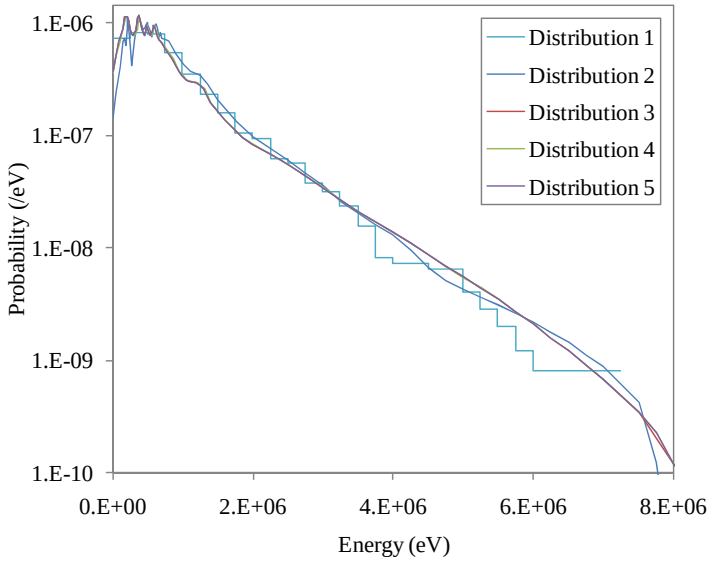


**Figure 1. Five fission photon emission spectra contained in the ENDF/B-VII.0 data.**

## 3. EXAMPLE PROBLEM

Many critical experiments were performed at the Oak Ridge Critical Experiments Facility (ORCEF), Building 9213 of the Y-12 Site, in the 1950s. Of the experiments carried out in this building, several consisted of stacked layers of $UF_4$/Teflon separated by thin cellulose acetate plastic moderator films. The layers could be stacked and sized during the approach to criticality. The building contained two large experimental bays and a variety of detectors and alarm systems.

To demonstrate the CAAS capability of SCALE, consider the following example problem based on one such critical assembly (Experiment 3), described in the International Criticality Safety Benchmark Evaluation Project (ICSBEP) collection of benchmark problems [12] and shown in Figure 2. It consisted of an unreflected stack of $UF_4$/Teflon layers (37.5% $^{235}U$), 5.08 cm thick, separated by thin sheets of cellulose acetate, 0.0254 cm thick. The typical slab of $UF_4$/Teflon was about 71 cm by 76 cm, with slightly smaller layers near the top. The topmost layer, the "penthouse," was only 15 cm by 25 cm. The entire experiment sat on a 2.54 cm thick aluminum base plate. The reported benchmark value for $k_{eff}$ was 0.99701±0.00464. Using KENO-V.a and the ENDF/B-V 238-group library with SCALE 5, the evaluators calculated $k_{eff}$ to be 1.01444±0.00010.

For this example, assume a criticality excursion involving $10^{18}$ total fissions. This example will use three MAVRIC calculations to find (a) the total dose at the detectors in the lower level of the control room, (b) the total dose at the detectors in the upper level of the west assembly room, and (c) the total dose on a mesh covering the inside and the areas just outside the experimental bay.

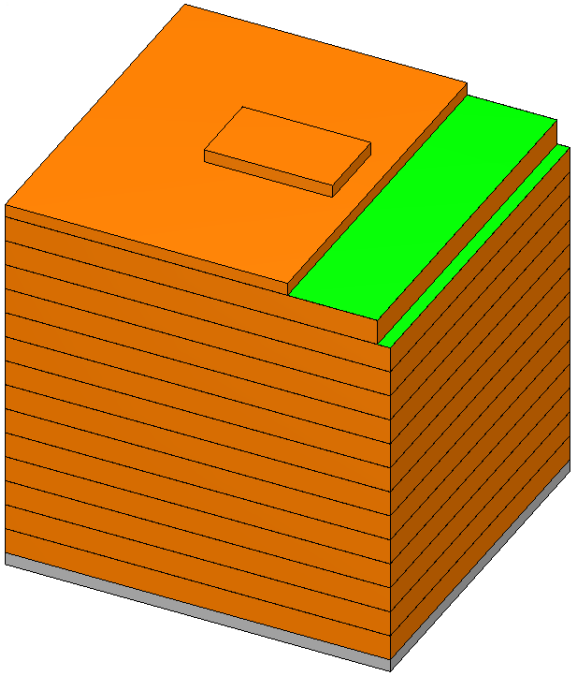

**Figure 2. Model of the unreflected stacked layer experiment.**

### 3.1 Part One – KENO Criticality and Fission Source Distribution

The model used for the above experiment from ICSBEP [12] was converted to a CSAS6 model using the ENDF/B-VII 238-group library. Just like the benchmark calculation, a total of 1,000 generations were used with 50 skip generations and 7,000 source particles per generation. The fission distribution was accumulated on a 13 × 12 × 10 mesh covering a cube 78 × 72 × 80 cm surrounding the fissionable material. Results from this 140-min calculation are shown in Table II. Note that the 1% difference in $k_{eff}$ compared to the benchmark value is due to the different cross-section libraries (which does not matter in this problem in finding the fission distribution). The calculated fission source distribution is shown in Figures 3 and 4.

**Table II. Results of the CSAS6 calculation**

| Quantity | | Value | Uncertainty |
|---|---|---|---|
| $k_{eff}$ | best estimate system k-eff | 1.02571 | 0.00010 |
| $\bar{\nu}$ | system nu bar | 2.49031 | 1.11E-05 |

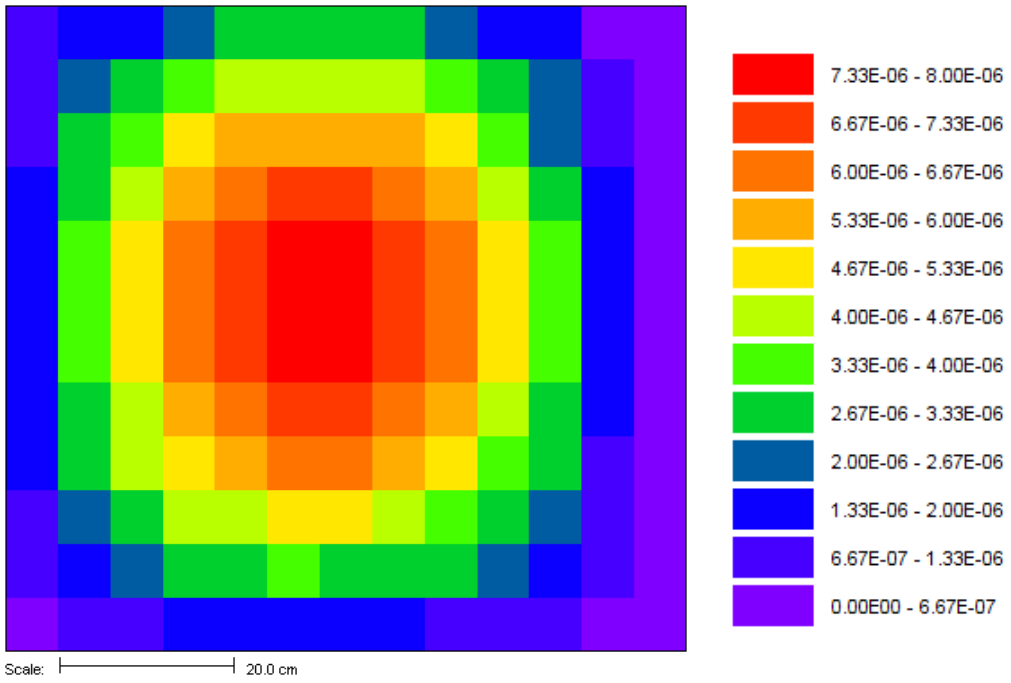


**Figure 3. Fission source spatial distribution for the center horizontal slice.**

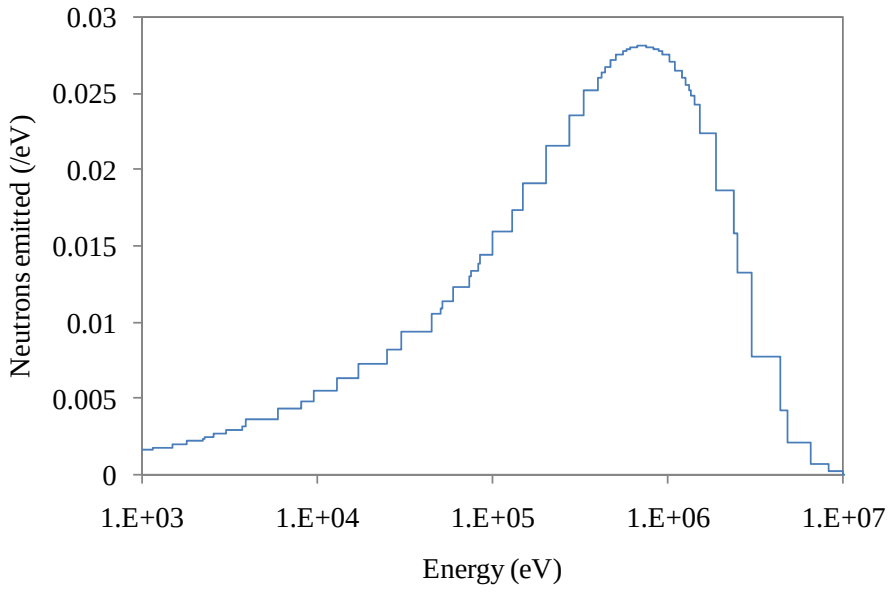


**Figure 4. Fission source energy distribution for the center voxel.**

## 3.2 Part Two – MAVRIC Transport Calculations

For the second part of the example problem, the critical assembly described above (Figure 2) can be placed inside a simple model of the west wing of ORCEF, shown in Figures 5 and 6. Here, only the west assembly room and its control room are included. Not included in this model are the offices, counting rooms, and another high bay (the east assembly room) that are located to the east (in the positive *x* direction). This model is for demonstration purposes only—the dimensions are estimates based on old drawings contained in the ICSBEP files [12,13] and an Oak Ridge Associated Universities technical report [14].

The walls, floors, and roof are concrete. The floor dividing the upper and lower levels is a grated steel walkway, modeled here as steel with a low volume fraction (10 lb/ft$^2$, which is a typical value for steel grate). The steel grating is 12 ft above the concrete floor of the high bay. A stairway in the northwest corner of the lower west assembly room is also modeled with steel grate. Two tanks in the lower west assembly and two tanks in the upper west assembly are modeled as empty steel shells. The lower tanks probably contained water used in the upper tanks for critical experiments. In the wall between the control room and the west assembly high bay are four water-filled windows, one on the lower level and three on the upper level. No information was given in these references about the detectors, other than an approximate location shown on a building schematic. The building sits on the side of a hill. Drawings hint that the hill slopes upward from the building's ground level on the north side.

The MAVRIC calculations used the fission distribution mesh source that was produced by KENO-VI. For the transport, the new ENDF/B-VII.0 27n/19g shielding library [11] was used, and the 238-group fission source was translated automatically by MAVRIC. The source strength was set to $6.9175 \times 10^{14}$, which is $10^{18}$ fissions per incident multiplied by the system $\bar{\nu}$ and divided by 3,600 s per h, so that the final tally results will be in rem per incident instead of the typical rem per hour when using source strength units of "per second." Fission photons were added to the source by using the distribution for $^{235}$U. The critical assembly model and the mesh source were placed about 30 cm above the steel grating floor of the upper level. For the importance maps in each MAVRIC calculation, a coarse mesh of about 60 × 60 × 40 voxels was defined over the entire model. The mesh planes included all of the significant material boundaries (walls, floors, tanks, etc.), planes to divide the source using the same spacing as the fission source distribution, and planes bounding the detectors (different in each case).

### 3.2.1. Lower level detectors

For calculation of doses seen by the detectors on the lower level of the control room, MAVRIC was optimized for transport of neutrons and photons to these detectors. First, MAVRIC used Denovo to calculate the adjoint fluxes from an adjoint source located over an area surrounding the three detectors using an energy spectrum corresponding to the flux-to-dose conversion factors for both neutron and photons. This adjoint $S_N$ solution required 20 min. From the adjoint fluxes, MAVRIC created the space- and energy-dependent weight window and source biasing parameters, which were then passed to the Monaco Monte Carlo code. The Monaco calculation ran for 8 h, and the final doses at the detectors are shown in Table III.

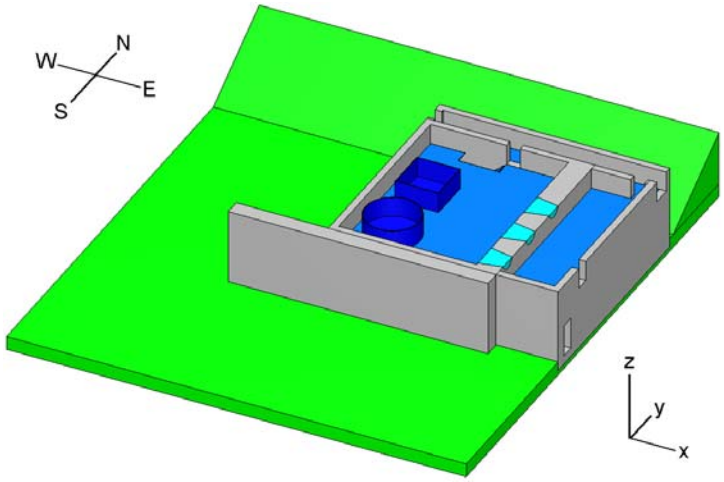


**Figure 5. Model of the west side of the Oak Ridge Critical Experiments Facility, with a cut-away view showing the upper level.**

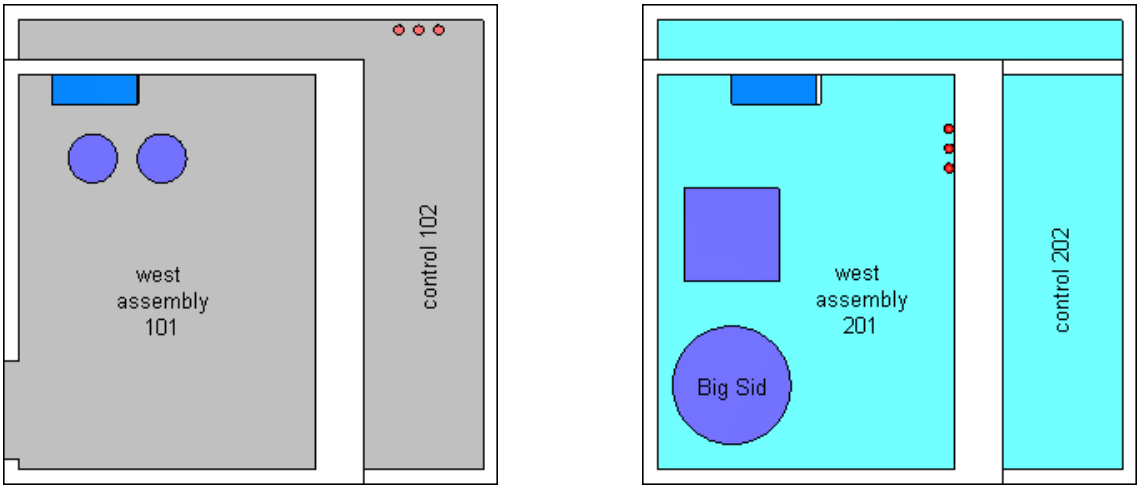


**Figure 6. Model of the Oak Ridge Critical Experiments Facility west assembly and control room lower level (left) and upper level (right) showing the locations of the detectors.**

**Table III. MAVRIC results (8.3 h) for the lower control room detectors**

| | Neutron | | Photon | | Total | |
|---|---|---|---|---|---|---|
| Detector | Value (rem) | Relative Uncertainty | Value (rem) | Relative Uncertainty | Value (rem) | Relative Uncertainty |
| **west** | 23.3 | 2.2% | 1.59 | 7.7% | 24.9 | 2.2% |
| **center** | 18.5 | 2.6% | 1.28 | 4.9% | 19.7 | 2.5% |
| **east** | 15.6 | 3.2% | 1.03 | 5.7% | 16.6 | 3.0% |

### 3.2.2. Upper level detectors

Table IV gives the results for the detectors on the upper level of the assembly room. Similar to the calculation described in Section 3.2.1, MAVRIC used an adjoint source covering all three detectors, ran an $S_N$ calculation, constructed an importance map and biased source, then ran Monaco. The Denovo adjoint calculation took 21 min and Monaco took 2 h.

**Table IV. MAVRIC results (2.3 h) for the upper assembly room detectors**

| | Neutron | | Photon | | Total | |
|---|---|---|---|---|---|---|
| Detector | Value (rem) | Relative Uncertainty | Value (rem) | Relative Uncertainty | Value (rem) | Relative Uncertainty |
| **south** | 19.2E+3 | 1.0% | 246 | 16.0% | 19.5E+3 | 1.0% |
| **center** | 16.5E+3 | 1.0% | 178 | 13.5% | 16.6E+3 | 1.0% |
| **north** | 14.6E+3 | 1.2% | 149 | 16.9% | 14.8E+3 | 1.2% |

Note that the uncertainties for the photon doses are much higher than those for the neutron doses. This is because the simulation was optimized for the calculation of total dose and the photon component of the total dose is only about 1%. Had a separate calculation been done that used an adjoint source of just the photon response, the photon dose rate uncertainties would have been much smaller but at the expense of the neutron dose rate.

### 3.2.3. Mesh tally of dose

The FW-CADIS option in MAVRIC was used for the calculation of the dose everywhere inside the ORCEF west assembly and just outside the west assembly. This option automatically did the following: First, a forward discrete ordinates calculation was done to estimate the doses everywhere. This was then used to weight the adjoint source strength, which was defined as a volume covering the building and the areas to the north, west, and south of the building. Finally, the resulting adjoint fluxes were used to create an importance map and biased source which were then used by Monaco. Calculation times for the MAVRIC components were 19 min for the forward Denovo, 18 min for the adjoint Denovo, and 2 h for Monaco. The final mesh tally is shown in Figure 7. The mesh tally was calculated with 91% of the voxels having less than 10% relative uncertainty. If lower uncertainties were required, the Monaco calculation could be run longer. FW-CADIS helps balance the calculation so that areas of high dose and low dose are computed with more uniform relative uncertainties. Note that the shield wall on the south side of the assembly area is doing its job well—reducing dose to south side (where there is a road leading to the building entrance) by a great deal compared to the west side. Most of the control room doses are between 0.25 rem and 2.5 rem.

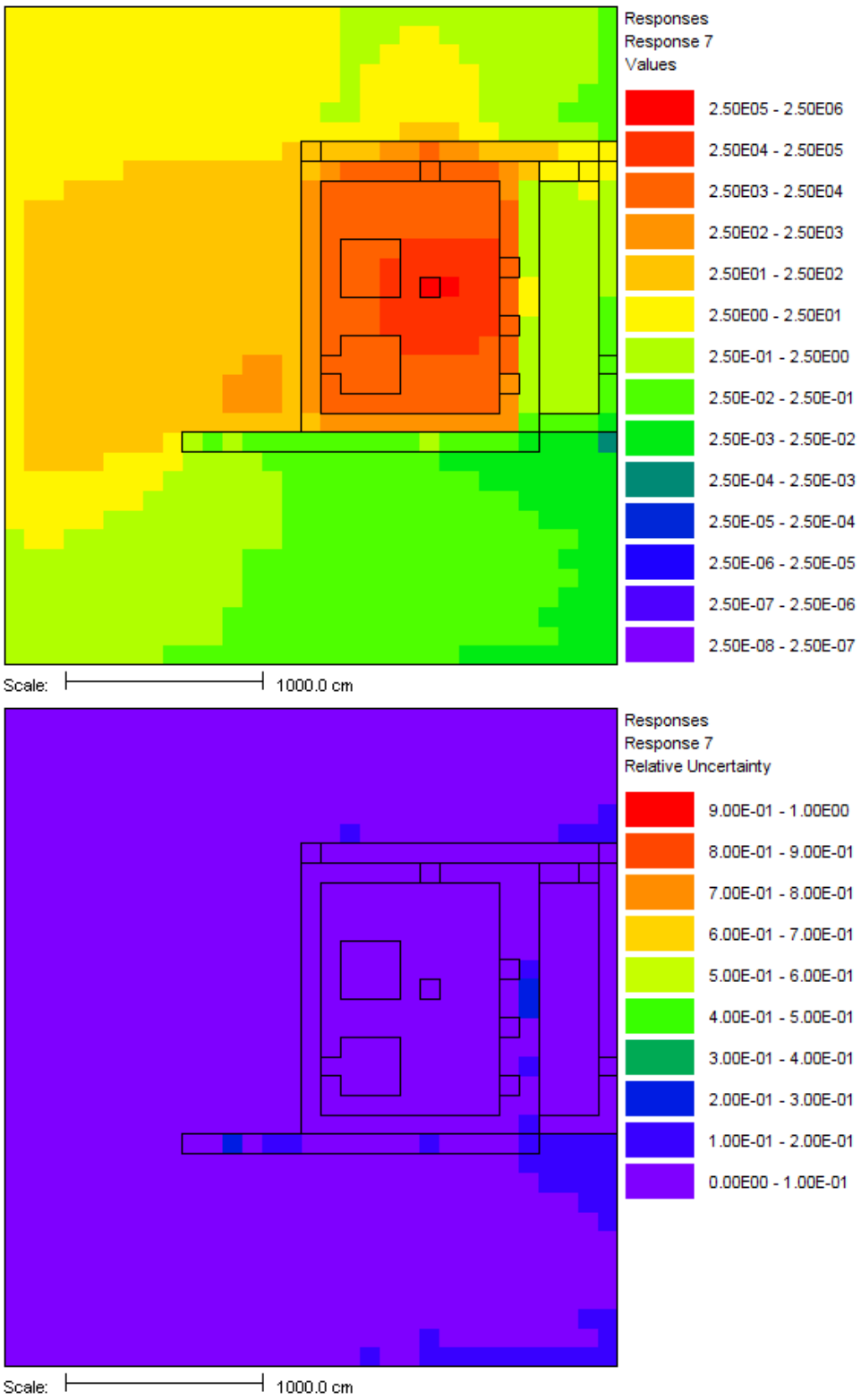


**Figure 7. Mesh tally showing (top) the total dose (rem) from the incident at the level of the critical experiment and (bottom) the relative uncertainty in each voxel.**

### 3.3. Analog Calculation

To show the effect of the automated variance reduction in MAVRIC, an analog calculation using the KENO-derived mesh source, but without any importance map or biased source distribution, was run for 180 h.

Table V shows the total doses from the analog calculation. For the detectors on the upper level (in the same room as the source), the total dose results matched well. Relatively few particles were transported to the detectors on the lower level, with doses a factor of ~1,000 less than the upper level detectors. The statistical uncertainties were too large to make a meaningful comparison to the CADIS dose results.

**Table V. Analog results (180 h) for detector doses**

| | | Total Dose | |
|---|---|---|---|
| | | Value | Relative |
| Level | Detector | (rem) | Uncertainty |
| lower | west | 12.1 | 33% |
| | center | 7.39 | 28% |
| | east | 15.1 | 35% |
| upper | south | 18.7E+03 | 4.7% |
| | center | 18.7E+03 | 4.8% |
| | north | 13.6E+03 | 5.2% |

The mesh tally had difficulty calculating the low dose areas. The large amount of statistical uncertainty is apparent in the contour plot shown in Figure 8. Even after 180 h, only 46% of the voxels had less than 10% relative uncertainty.

For the upper level detectors, using the CADIS option in MAVRIC resulted in an increase in the figure-of-merit (FOM) compared to analog by a factor of ~1500. For the harder problem of the doses at the lower level detectors, the automated variance reduction increased the FOM by a factor of 3000-4500 compared to the analog calculation. This is typical of CADIS—harder problems benefit even more dramatically.

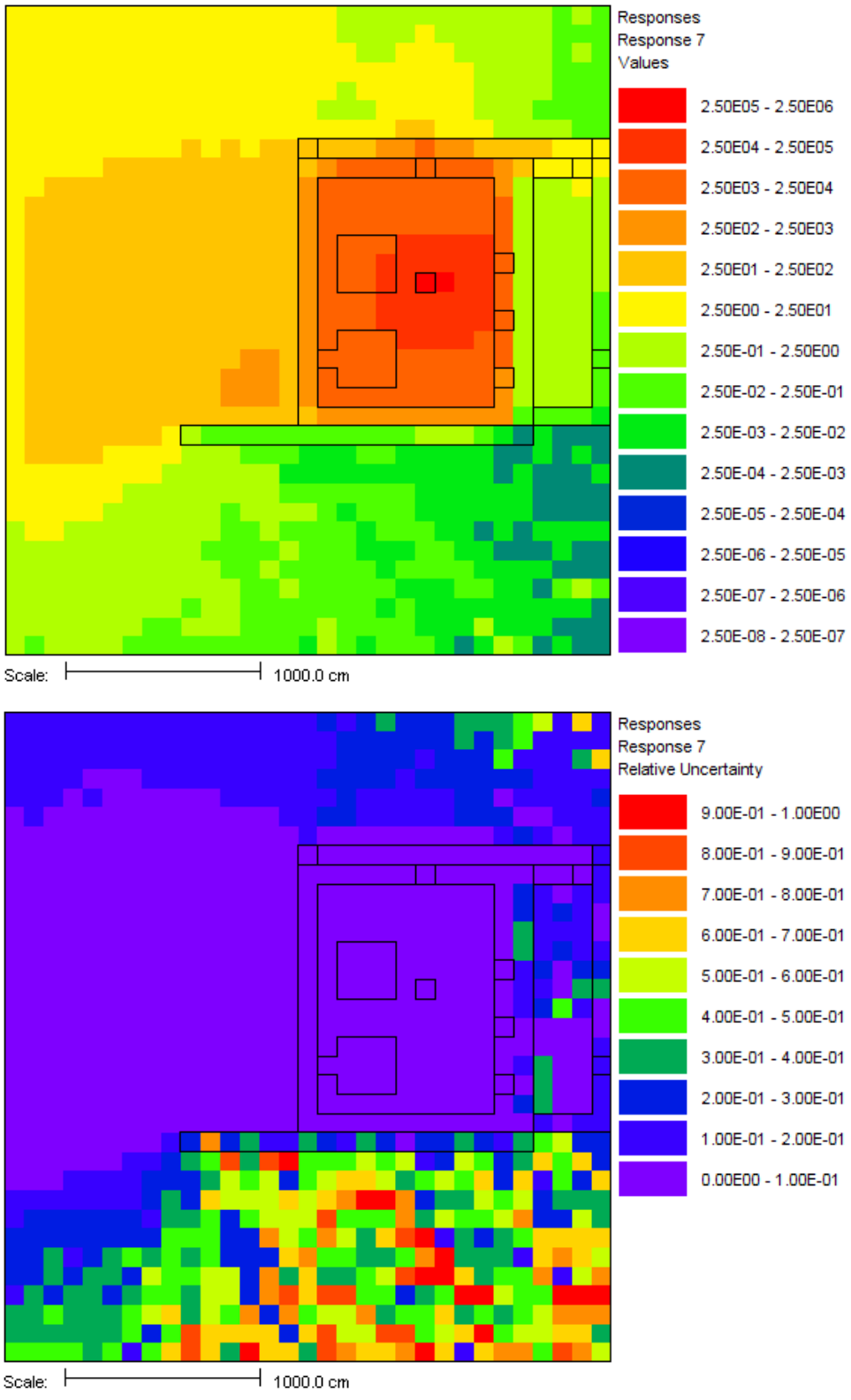


**Figure 8. Analog mesh tally showing (top) the total dose (rem) from the incident at the level of the criticality experiment and (bottom) the relative uncertainty in each voxel.**

## 4. CONCLUSIONS

SCALE 6 has the capability to do detailed simulations of criticality accident alarm systems. The automated variance reduction capabilities of the MAVRIC radiation transport sequence allow for the full three-dimensional analysis of CAAS problems in reasonable amounts of computer time. This advantage in speed also allows for the use of the three-dimensional fission source distribution that can be determined by the KENO-VI criticality code. The fission spatial/energy distribution and the critical assembly itself can be included in the transport model.

## ACKNOWLEDGMENTS

The authors would like to thank the Division of Fuel Cycle Safety and Safeguards of the U.S. Nuclear Regulatory Commission for funding this work. Thanks also go to Bryan L. Broadhead for providing background material and suggestions for the manuscript.

Oak Ridge National Laboratory is managed and operated by UT-Battelle, LLC, for the U.S. Department of Energy under Contract No. DE-AC05-00OR22725.

## REFERENCES

1. R. M. Westfall and J. R. Knight, “Radiation Levels in a Gaseous Diffusion Plant Assuming a Low-Enriched Criticality Event Corresponding to the ANSI-Standard Minimum Accident of Concern,” Oak Ridge Gaseous Diffusion Plant, K/CSD/TM-55, 1984.
2. B. L. Broadhead, R. L. Childs, R. M. Westfall, and C. V. Parks, *Evaluation of Criticality Alarm Response and the WEMCO Fernald Site*, ORNL/TM-12232, Oak Ridge National Laboratory, Oak Ridge, Tenn., November 1992.
3. J. C. Wagner, “Acceleration of Monte Carlo Shielding Calculations with an Automated Variance Reduction Technique and Parallel Processing,” Ph.D. Dissertation, Pennsylvania State University, University Park, Pennsylvania, 1997.
4. A. Haghighat and J. C. Wagner, “Monte Carlo Variance Reduction with Deterministic Importance Functions,” *Progress in Nuclear Energy*, **42(1),** 25–53, (2003).
5. J. C. Wagner and A. Haghighat, “Automated Variance Reduction of Monte Carlo Shielding Calculations Using the Discrete Ordinates Adjoint Function,” *Nuclear Science and Engineering*, **128**, 186 (1998).
6. D. E. Peplow, S. M. Bowman, J. E. Horwedel, and J. C. Wagner, “Monaco/MAVRIC: Computational Resources for Radiation Protection and Shielding in SCALE,” *Transactions of the American Nuclear Society* **95**, 669–671 (2006).
7. D. E. Peplow, E. D. Blakeman, and J. C. Wagner, “Advanced Variance Reduction Strategies for Optimizing Mesh Tallies in MAVRIC,” *Transactions of the American Nuclear Society*, **97**, 595–597 (2007).
8. D. E. Peplow and J. C. Wagner, “Simultaneous Optimization of Tallies in Difficult Shielding Problems,” pp. 29 in *Proc. of the 11th International Conference on Radiation Shielding (ICRS-11) and the 15th Topical Meeting of the Radiation Protection and Shielding Division (RPSD-2008) of the American Nuclear Society*, April 14–18, 2008, Pine Mountain, Georgia.

9. J. C. Wagner, E. D. Blakeman, and D. E. Peplow, "Forward-Weighted CADIS Method for Global Variance Reduction," *Transactions of the American Nuclear Society,* **97**, 530–633 (2007).
10. E. D. Blakeman, D. E. Peplow, J. C. Wagner, B. D. Murphy, and D. E. Mueller, *PWR Facility Dose Modeling Using MCNP5 and the CADIS/ADVANTG Variance-Reduction Methodology*, ORNL/TM-2007/133, Oak Ridge National Laboratory, Oak Ridge, Tenn., September 2007.
11. D. Wiarda, M. E. Dunn, D. E. Peplow, T. M. Miller, and H. Akkurt, *Development and Testing of ENDF/B-VI.8 and ENDF/B-VII.0 Coupled Neutron-Gamma Libraries for SCALE 6*, ORNL/TM-2008/047 (in press, 2008).
12. K. R. Elam, D. F. Hollenbach, and W. C. Jordan, "Unreflected $UF_4$-$CF_2$ Blocks with 37.5% $^{235}U$" (IEU-COMP-INTER-003), *International Handbook of Evaluated Criticality Safety Benchmark Experiments, Volume III - Criticality Alarm/Shielding Benchmarks*, NEA/NSC/DOC/(95)03/III, Organization for Economic Co-operation and Development - Nuclear Energy Agency (OECD-NEA) (September 2007).
13. K. R. Elam, W. C. Jordan, L. L. Gilpin, C. M. Hopper, and R. M. Lell, "Paraffin-Reflected 5-, 5.4-, 5-, 6.6-, 7.5-, 8-, 8.5-, 9-, and 12-Inch-Diameter Cylinders of $^{233}U$ Uranyl Fluoride Solutions" (U233-SOL-THERM-003), *International Handbook of Evaluated Criticality Safety Benchmark Experiments, Volume V - Criticality Alarm/Shielding Benchmarks*, NEA/NSC/DOC/(95)03/V, Organization for Economic Co-operation and Development - Nuclear Energy Agency (OECD-NEA) (September 2007).
14. G. D. Kerr, E.L. Frome, W.G. Tankersley, and J.P. Watkins, *Historical Evaluation of the Film Badge Dosimetry Program at the Y-12 Facility in Oak Ridge, Tennessee Part 2 – Neutron Radiation*, Oak Ridge Associated Universities Technical Report #2004-1406.